Pediatr Nephrol (2010) 25:1063–1072
DOI 10.1007/s00467-009-1437-x

ORIGINAL ARTICLE

A comparative proteomic study of nephrogenesis in intrauterine growth restriction

Qian Shen · Hong Xu · Li-Ming Wei · Jing Chen · Hai-Mei Liu · Wei Guo

Received: 10 September 2009 / Revised: 17 December 2009 / Accepted: 29 December 2009 / Published online: 4 February 2010

Abstract Nephrogenesis requires a fine balance of many factors that can be disturbed by intrauterine growth restriction (IUGR), leading to a low nephron endowment. The aim of this study was to test the hypothesis that IUGR affects expression of key proteins that regulate nephrogenesis, by a comparative proteomic approach. IUGR was induced in Sprague–Dawley (SD) rats by isocaloric protein restriction in pregnant dams. A series of methods, including two-dimensional gel electrophoresis (2-DE), silver staining, mass spectrometry and database searching was used. After silver staining, 2-DE image analysis detected an average 730±58 spots in the IUGR group and 711±73 spots in the control group. The average matched rate was 86% and 81%, respectively. The differential proteomic expression analysis found that 11 protein spots were expressed only in the IUGR group and one in the control group. Seven protein spots were up-regulated more than fivefold and two were down-regulated more than fivefold in the IUGR group compared with those in control group. These 21 protein spots were preliminarily identified and were structural molecules, including vimentin, perlecan, gamma-actin and cytokeratin 10, transcription regulators, transporter proteins, enzymes, and so on. These proteins were involved primarily in energy metabolism, oxidation and reduction, signal transduction, cell proliferation and apoptosis. Data from this study may provide, at least partly, evidence that abnormality of metabolism, imbalance of redox and apoptosis, and disorder of cellular signal and cell proliferation may be the major mechanisms responsible for abnormal nephrogenesis in IUGR.

Keywords Intrauterine growth restriction · Kidney · Proteomics · Vimentin · Perlecan

Q. Shen · H. Xu (✉) · J. Chen · H.-M. Liu · W. Guo
Department of Nephrology and Rheumatology,
Children's Hospital of Fudan University,
399 Wan Yuan Road, Minhang District,
Shanghai 201102, People's Republic of China
e-mail: hxu@shmu.edu.cn

L.-M. Wei
Institutes for Biomedical Sciences, Fudan University,
Shanghai, People's Republic of China

Introduction

Intrauterine growth restriction (IUGR) has long-term effects on various organisms through fetal programming [1, 2]. Human studies of the association between IUGR and renal diseases indicate that, in contrast to the normal fetal kidney, the IUGR fetal kidney has less volume, with a significant reduction in the number of glomeruli [3, 4]. In addition, long-term follow-up after birth showed that there was significantly lower glomerular filtration and greater incidence of proteinuria in the IUGR group than in the control group [5, 6]. Our previous animal studies have also shown a decrease in the number of glomeruli in IUGR rats, with an increased incidence of proteinuria and hypertension in the postnatal follow-up period [7]. However, the mechanism underlying IUGR-induced abnormal nephrogenesis has not yet been fully clarified.

We investigated the differences in proteomic profiles between normal and IUGR neonatal rats in order to identify the key proteins that are associated with nephrogenesis in IUGR rats.

Materials and methods

This work was performed with the approval of the Children's Hospital of Fudan University's Institutional Animal Use and Care Committee.

Establishment of the IUGR animal model

Twelve female Sprague–Dawley (SD) rats (Clean conventional animals, body weight 250–300 g, provided by the Department of Experimental Animals, Fudan University, Shanghai, China) were randomly divided into two groups after mating with male rats. The normal control group was supplied with conventional feed (22% protein) during the gestation period until they underwent natural labor. The resulting neonatal rats were assigned to the control group. To establish the IUGR animal model, we provided a low-protein isocaloric diet, consisting of 6% protein, to the IUGR group throughout the entire pregnancy period until natural labor [8]. The resulting newborn rats with body weights two standard deviations below the average were assigned to the neonatal IUGR rats (IUGR group).

Measurement of kidney weight and glomerular count

Sixteen newborn male rats were selected from each group. The rats were killed by jugular puncture after being anesthetized. The kidney weight and body weight of the rats in each group were measured. The kidneys were conventionally fixed, embedded, sliced, and stained with hematoxylin and eosin (HE). The glomeruli were counted. The method for counting the glomeruli has been previously reported [9, 10].

Two-dimensional gel electrophoresis and image analysis

Eight neonatal IUGR kidneys (average weight 48±4 mg/kidney, total weight 385 mg) and six neonatal normal kidneys (average weight 64±4 mg/kidney, total weight 383 mg) were mixed for total protein extraction. Tissues were homogenized in a lysis buffer, spun down to collect the supernatant, and subjected to the Bradford assay to determine protein concentration. Two-dimensional gel electrophoresis (2-DE) was performed according to the manufacturer's instructions (Amersham Biosciences, Buckinghamshire, UK). Immobiline pH gradient DryStrip gel (18 cm, non-linear pH 3~10, Amersham Biosciences) was rehydrated with 450 μl of re-swelling buffer containing 250 μg protein sample at 20°C for 12 h, focused by gradient-increasing voltage to 8,000 V, and continued until a total of 52,000 voltage-hours was reached. After focusing, the strip was equilibrated for 15 min in an equilibration solution containing 1% dithiothreitol and 2.5% iodine acetamide and transferred to the top of a 12.5% polyacrylamide gel for sodium dodecyl sulfate–polyacrylamide gel electrophoresis (SDS-PAGE). The electrophoresis was performed at 25°C until bromophenol blue reached the bottom of the gel. The gel was stained by silver stain and then scanned for image analysis. Each 2-DE experiment was performed in triplicate to confirm the reproducibility. The scanned gel images were then analyzed by software PDQuest 7.3.0 (Bio-Rad, Hercules, CA, USA).

In-gel digestion and mass spectrometry

Protein spots with significant differences between the two groups were excised from the gels and placed into a 96-well micro-titer plate. The gel pieces were put into a solution of 15 mM potassium ferricyanide and 50 mM sodium thiosulfate (1:1) for 20 min at room temperature. Then they were washed twice with deionized water and dehydrated in acetone cyanohydrin (ACN). The samples were then rehydrated in a digestion buffer containing 20 mM ammonium bicarbonate and 12.5 ng/μl trypsin (Roche, Indianapolis, IN, USA) at 4°C. After 30 min incubation, the gels were digested for more than 12 h at 37°C. The peptides were then extracted twice with 0.1% trifluoroacetic acid (TFA) in 50% ACN. The extracts were dried under the protection of nitrogen (N_2).

For matrix-assisted laser desorption ionization–time of flight mass spectrometry (MALDI-TOF-MS), the peptides were eluted onto the target with a 0.7 μl matrix solution (α-cyano-4-hydroxy-cinnamic acid in 0.1% TFA and 50% ACN). Then, the solution was spotted onto a stainless steel target with 192 wells (Applied Biosystems, Framingham, MA, USA). The samples were allowed to dry in air before being inserted into the mass spectrometer. The MALDI mass spectrometer was an ABI 4700 TOF-TOF proteomics analyzer (Applied Biosystems). The ultraviolet (UV) laser was operated at a 200 Hz repetition rate and a wavelength of 355 nm. The accelerated voltage was operated at 20 kV. The data were searched by GPS Explorer (Applied Biosystems) using MASCOT as a search engine. Data from MALDI-TOF tandem mass spectrometry (MS/MS) were analyzed using MASCOT (Matrix Science, London, UK) search software. The following parameters were used in the search: retrieval species for rat, enzyme for trypsin, missed cleavage by 1, peptide tolerance of 0.2, MS/MS tolerance of 0.6 Da and possible oxidation of methionine.

Western blot

Two sets of kidney tissue lysates from both the IUGR and control groups were subjected to Western blotting. Conventionally, 40 μg of total protein was first separated by 12% SDS-PAGE and transferred to a polyvinylidene fluoride (PVDF) membrane by semi-dry transfer, and the membrane was blocked in 5% non-fat milk at room temperature for 1 h. The membrane was then incubated with monoclonal mouse anti-vimentin antibody (1:400, Abcam, Cambridge, UK) or monoclonal anti-perlecan antibody (1:500, Biomeda, CA, USA) at 4°C overnight,

followed by incubation with horseradish peroxidase (HRP)-labeled secondary antibody (1:2000, Abcam) at room temperature for 1 h. The protein was visualized by enhanced chemiluminescence (ECL), and glyceraldehyde-3-phosphate dehydrogenase (GAPDH) (Kangchen, Shanghai, China) was detected as the internal control.

Immunohistochemistry

Three kidney tissue sections from either the IUGR or the control group were used for the detection of the expression level of vimentin or perlecan by immunohistochemical staining. Paraffin-embedded tissue sections were first dewaxed and rehydrated. Microwave antigen retrieval was done in the presence of citric acid buffer (pH 6.0). The samples were blocked with horse serum for 20 min before incubation with monoclonal mouse anti-vimentin antibody (1:100, Abcam) or monoclonal anti-perlecan antibody (1:100, Biomeda) at 37°C for 1 h, followed by incubation at 4°C overnight. The tissue sections were then incubated with biotin-labeled secondary antibody (Kangchen) or phosphate-buffered saline (PBS) solution for the negative control at 37°C for 1 h and chromogenized by diamino-benzidine (DAB). Nuclei were counterstained with hematoxylin.

Statistical analysis

Quantitative data were presented as means ± standard deviations. Comparisons between groups were made with the least significant difference (LSD) test. P values less than 0.05 were considered to be statistically significant.

Results

Comparison of kidney weight and number of glomeruli at birth The kidney weight and the ratio of kidney weight to body weight in the IUGR group were lower than those in the control group ($P<0.001$) (Table 1). The number of glomeruli in the IUGR group (number/unilateral kidney) was significantly lower than that in control group (IUGR group 22,891±1242; control group 28,466±919, $P<0.001$).

Table 1 Comparison of kidney weights at birth. Data are means ± standard deviations; $n=16$ per group

Parameter	Control group	IUGR group
Body weight (g)	6.920±0.329	4.810±0.272*
Kidney weight (g)	0.065±0.004	0.038±0.003*
Kidney weight/body weight (%)	0.945±0.025	0.785±0.041*

*Compared with control group, $P<0.001$

Comparison of renal tissue morphology at birth Hematoxylin and eosin (HE) staining showed that the cortex in the IUGR group was significantly thinner than that in control group (IUGR group 391.94±24.73 μm; control group 425.50±24.01 μm, $P<0.01$), while the nephrogenic zone in the IUGR group was significantly thicker than that in the control group (IUGR group 149.26±13.92 μm; control group 109.22±27.06 μm, $P<0.05$).

Results of 2-DE and mass spectrometry

Total proteins were extracted from the kidneys of eight IUGR and six normal control neonatal rats and then subjected to 2-DE three times to show reproducibility. Three sets of 2-DE profiles were obtained (Fig. 1). With the application of PDQuest 7.3.0 software for image analysis, these results showed that a total of 730±58 protein spots was obtained in the IUGR group, with an average match rate of 86%. A total of 711±73 protein spots was obtained from the control group, with an average match rate of 81%. The differential expression analysis found that 11 protein spots were expressed only in the IUGR group (nos. 1–11) and one spot only in the control group (no. 12). Seven protein spots were up-regulated more than fivefold (nos. 13–19), and two spots were down-regulated more than fivefold (nos. 20 and 21) in the IUGR group compared with those in the control group. These 21 protein spots were picked for mass spectrometry analysis, and all were successfully identified (Table 2).

Retrieval and classification of different protein functions

We used the gene ontology (GO) classification method for functional analysis of the 21 proteins, focusing on biological process, cellular component, and molecular function (Table 3). These proteins are involved primarily in energy metabolism, oxidation and reduction, signal transduction, cell proliferation and apoptosis.

Structural molecules accounted for 20% of the identified proteins and included vimentin, perlecan, gamma-actin, cytokeratin 10, transcription regulators such as the splicing factor (arginine/serine-rich 9), Rho guanosine diphosphate (Rho GDP) dissociation inhibitor alpha, cell division protein kinase 2 as well as transporter proteins and enzymes.

Confirmation of vimentin expression by Western blot and immunohistochemistry

Western blot results showed that vimentin expression level was significantly higher in the IUGR group than in the control group (Fig. 2). Brown granules in the immunohis-

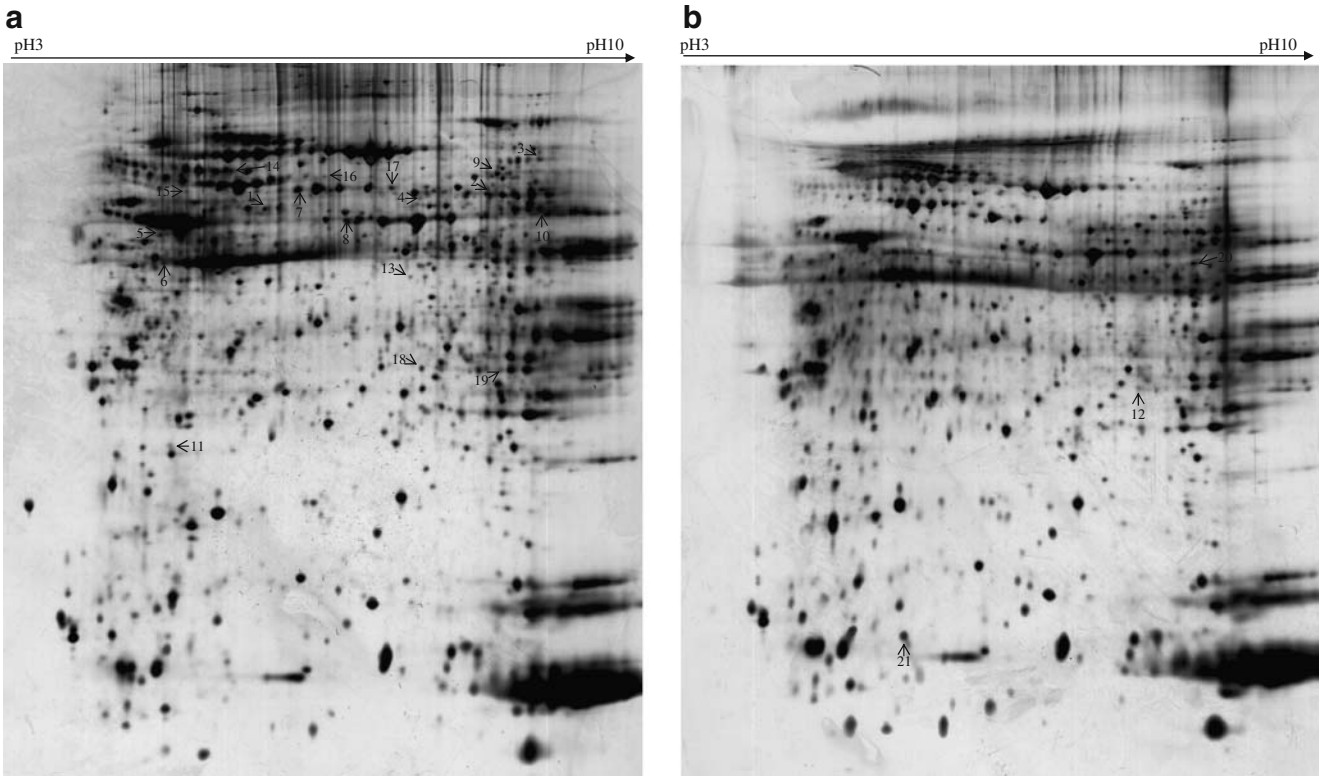

Fig. 1 Images of the 2-DE profiles. **a** IUGR group; **b** control group. Locations of 21 differentially expressed protein spots. The numbers of the protein spots correspond to those listed in Table 2

tochemical staining revealed the distribution of vimentin after DAB chromogenization. Immunohistochemistry (IHC) result indicated that vimentin was expressed primarily in glomeruli, and its expression was significantly increased in the IUGR group compared to the control group (Fig. 3).

Confirmation of perlecan expression by Western blot and IHC

Western blot results showed that the perlecan expression level was significantly lower in the IUGR group than in the control group (Fig. 4). Brown granules in the immunohistochemical staining revealed the distribution of perlecan after DAB chromogenization. IHC results indicated that perlecan was expressed in both the glomeruli and the tubules, and the level of perlecan was significantly reduced in the IUGR group compared to the control group (Fig. 5).

Discussion

IUGR may have a long-term impact on organ function through the process of fetal programming. IUGR causes hormone imbalance and metabolic disorders, affects growth and development in many organs, and is associated with many diseases that can jeopardize human health, such as hypertension, coronary heart disease, diabetes and chronic kidney disease [11, 12].

Our results in SD rats showed that the offspring born to mothers fed on low protein diets during pregnancy had fewer glomeruli than normal at birth. The cortex in the IUGR group was significantly thinner, while the nephrogenic zone was significantly thicker, than those in the control group. However, until now, apart from some studies that revealed increased apoptosis in the developing kidney and changes in the renin–angiotensin system, the detailed pathogenic mechanism of abnormal nephrogenesis has been largely unknown [13–16]. Studies on how IUGR affects nephrogenesis may contribute to our understanding of the pathogenesis of renal diseases related to fetal origin and may uncover potential therapeutic targets.

Proteomic technology has been used extensively in basic medical research in the past few years. It has been used to study systemic and quantitative proteomic changes in tissues and cells at different stages of disease progression. This is very important when disease pathogenesis is being studied and when new drug targets are being searched for. In the field of kidney research, proteomic approaches have been used to compare the differences in protein expression profiles between the renal cortex and medulla [17]. At the same time, this technology has been applied to pathogenic studies in diabetic nephropathy, focal segmental glomerular

Table 2 Differentially expressed protein spots in the kidneys of newborn rats

Number	Name	MW	pI	Score	Sequence coverage (%)
1	Non-specific dipeptidase	52,767	5.43	132	33
2	Methylmalonate semialdehyde dehydrogenase	57,808	7.54	92	33
3	Transketolase	67,644	7.22	125	29
4	Uridine monophosphate synthetase	52,292	6.17	190	32
5	Vimentin	53,733	5.06	368	63
6	Apolipoprotein A-IV	44,456	5.06	232	60
7	Cytokeratin 10	59,511	5.13	184	21
8	26 S protease regulatory subunit 7	48,648	5.72	268	62
9	Delta-1-pyrroline-5-carboxylate dehydrogenase	61,811	7.70	160	16
10	Retinal dehydrogenase 1	54,459	7.94	152	32
11	Rho GDP dissociation inhibitor alpha	23,407	5.12	146	48
12	Splicing factor, arginine/serine-rich 9	25,498	8.67	78	45
13	Uroporphyrinogen decarboxylase	40,453	6.35	126	29
14	Heterogeneous nuclear ribonucleoprotein K	50,976	5.39	171	39
15	75 kDa glucose regulated protein	73,858	5.51	206	33
16	227 kDa spindle and centromere associated protein	227,218	5.47	95	21
17	Disulfide-isomerase A3	57,043	5.88	150	41
18	Cell division protein kinase 2	33,999	8.80	67	19
19	Alpha-electron transfer flavoprotein	35,009	8.62	391	48
20	Gamma-actin	41,832	5.22	161	24
21	Perlecan	398,294	5.85	145	20

MW molecular weight, *pI* isoelectric point, *GDP* guanosine diphosphate

sclerosis, lupus nephritis, tumors, and acute rejection [18–20]. However, due to limitations in sample quantity in both animal and clinical studies, 'sample pooling', by the mixing together of three to ten samples with the same background, before the 2-DE analysis has become a popular technique [21–23]. The results have suggested that analysis of mixed samples not only helps to reduce the required number of repeat runs in 2-DE but also reduces the standard deviation obtained from individual samples.

We applied sample pooling to study differential protein expression profiles between neonatal IUGR and control rats. Our results revealed that a total of 21 proteins showed significant differences in the expression profile. Functional classification of these differential proteins showed that they were involved primarily in biological processes such as energy metabolism, oxidation and reduction, signal transduction, cell proliferation and apoptosis. Meanwhile, structural molecules accounted for 20% of the differential proteins identified and included vimentin, perlecan, gamma-actin and cytokeratin 10.

Vimentin is the major intermediate filament protein of mesenchymal cells and has been implicated in multiple biological pathways. It is associated with apoptosis, inflammation, and homeostasis [24]. Previous studies have shown that vimentin expression is altered in different kidney diseases: prenatally detected hydronephrosis with chronic interstitial nephropathy in a biopsy exhibits greater immunostaining for vimentin, the expression of which positively correlates with renin, angiotensin II receptors 1 and 2 mRNA levels [25]. Meanwhile, vimentin expression increases rapidly in diabetic rats and patients with chronic glomerulonephritis [26, 27]. Kim et al. and Zou et al. have reported that puromycin aminonucleoside injection can cause extreme podocyte hypertrophy and increased glomerular size. At the same time, vimentin transcripts significantly increased [28, 29]. A recent study has shown that there was an increase in glomerular diameter in 3-month-old rats that underwent 50% intrauterine food restriction and that vimentin levels were higher in the tubulointerstitial areas than in control rats [30]. Our result was consistent with that and showed that vimentin was significantly increased in the IUGR group when compared with that in the control group. The function of intermediate filament proteins is primarily to increase the mechanical resistance of cells, and vimentin is an indicator of cell regeneration suggestive of recent injury. It is, therefore, tempting for one to speculate that the up-regulation of vimentin allows resident renal cells to progress to cell hypertrophy and increase the mechanical stability of the cytoskeletal network, which is suitable for renal growth.

Perlecan is a large multi-domain extracellular matrix proteoglycan that plays a crucial role in tissue development

Table 3 Function of differentially expressed proteins

Number	Name	Biological process	Cellular component	Molecular function
1	Non-specific dipeptidase	proteolysis	–	carboxypeptidase activity; metalloprotease activity; dipeptidase activity; protein dimerization activity; zinc ion binding
2	Methylmalonate semialdehyde dehydrogenase	beta-alanine catabolic process; oxidation reduction; thymine catabolic process; valine catabolic process;	mitochondrion	acyl-CoA binding; malonate-semialdehyde dehydrogenase activity; thiol-ester hydrolase activity
3	Transketolase	ribose phosphate biosynthetic process; pentose-phosphate shunt	endoplasmic reticulum membrane; microsome; peroxisome; soluble fraction	calcium ion binding; magnesium binding; monosaccharide binding; thiamin pyrophosphate binding; transketolase activity
4	Uridine 5′-monophosphate synthetase	de novo pyrimidine basic biosynthetic process; nucleoside metabolic process	–	orotate phosphoribosyltransferase activity; orotidine-5′-phosphate decarboxylase activity
5	Vimentin	–	cytoplasm; nuclear matrix; type III intermediate filament	protein kinase binding; structural constituent of cytoskeleton
6	Apolipoprotein A-IV	lipid transport; lipoprotein metabolic process; response to food	chylomicron	lipid binding; lipid transporter activity
7	Cytokeratin 10	epidermis development	intermediate filament	protein binding; structural constituent of epidermis
8	26 S protease regulatory subunit 7	–	cytosol; nucleus	ATP binding; protein binding
9	Delta-1-pyrroline-5-carboxylate dehydrogenase	oxidation reduction; proline biosynthetic process	mitochondrial matrix	1-pyrroline-5-carboxylate dehydrogenase activity
10	Retinal dehydrogenase 1	oxidation reduction	cytoplasm	retinal dehydrogenase activity; 3-chloroallyl aldehyde dehydrogenase activity
11	Rho GDP dissociation inhibitor alpha	Rho protein signal transduction; regulation of protein localization	cytoplasm; immunological synapse	GTPase activator activity; Rho GDP dissociation inhibitor activity; protein binding
12	Splicing factor, arginine/serine-rich 9	RNA splicing; mRNA processing	nucleus	RNA binding; nucleotide binding
13	Uroporphyrinogen decarboxylase	heme biosynthetic process	cytoplasm	uroporphyrinogen decarboxylase activity
14	Heterogeneous nuclear ribonucleoprotein K	RNA splicing; mRNA processing	cytoplasm; spliceosome	RNA binding; protein binding
15	75 kDa glucose regulated protein	protein folding	mitochondrion	ATP binding; unfolded protein binding
16	227 kDa spindle and centromere associated protein	cell division; meiosis; mitosis	centrosome; condensed chromosome kinetochore; spindle	–
17	Disulfide-isomerase A3	cell redox homeostasis	endoplasmic reticulum; endoplasmic reticulum lumen; melanosome	protein disulfide isomerase activity
18	Cell division protein kinase 2	cell division; mitosis; amino acid phosphorylation	–	ATP binding; cyclin-dependent protein kinase activity
19	Alpha-electron transfer flavoprotein	electron transport chain; transport	mitochondrial electron transfer flavoprotein complex	FAD binding; electron carrier activity
20	Gamma-actin	–	cytoplasm; cytoskeleton	ATP binding; protein binding
21	Perlecan	cell adhesion; chondrocyte differentiation; embryonic skeletal system morphogenesis; extracellular matrix organization; protein localization	basal lamina	protein binding

CoA coenzyme A, *ATP* adenosine triphosphate, *GTP* guanosine triphosphate, *GDP* guanosine diphosphate, *FAD* flavin adenine dinucleotide

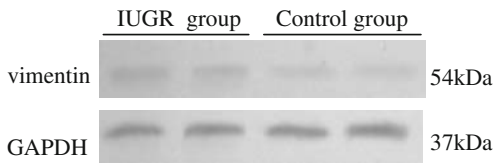

Fig. 2 Western blot analysis of vimentin expression in the kidneys. The expression of vimentin in the IUGR group was greater than that in the control group

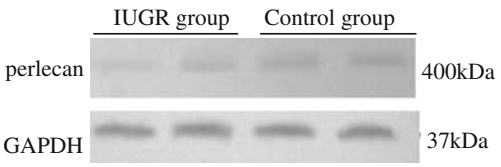

Fig. 4 Western blot analysis of perlecan expression in the kidneys. The expression of perlecan in the IUGR group was lower than that in the control group

and organogenesis, and it supports various biological functions, including cell adhesion and modulation of apoptosis. Meanwhile, perlecan also binds with relatively high affinity to a number of growth factors and surface receptors, thereby stabilizing cell–matrix links [31]. In normal kidneys, perlecan plays an important role in the maintenance of the glomerular filtration barrier. Perlecan null mice display abnormal early embryonic or perinatal lethality. The histological examination of these mice shows a marked disorganization in the structure and architecture of the developing tissue [32]. A down-regulation of perlecan has been reported in rats with puromycin aminonucleoside-induced nephrosis [33]. Mean-

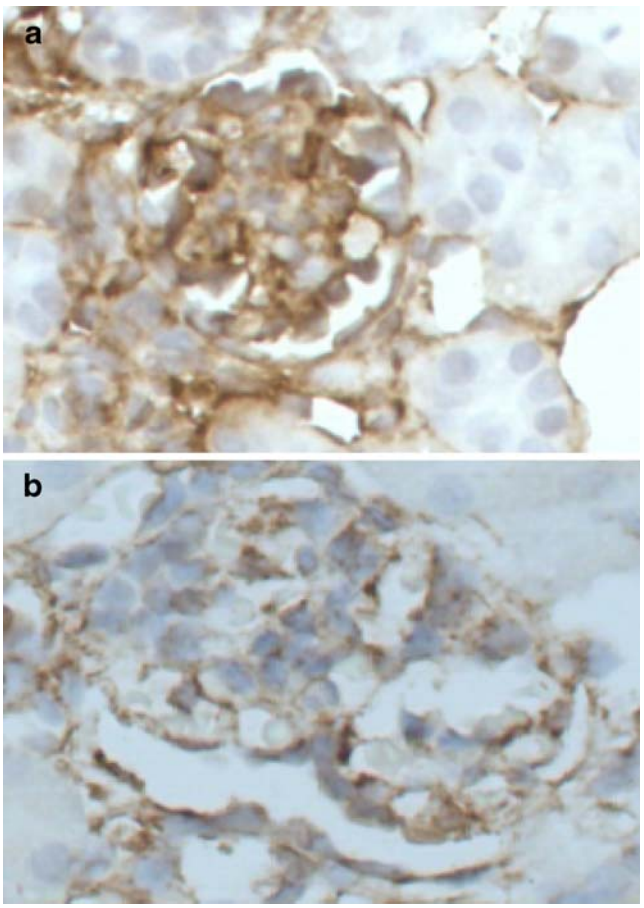

Fig. 3 IHC analysis of vimentin expression in the kidneys. **a** IUGR group; **b** control group. Vimentin was primarily expressed in the glomeruli. The staining in the IUGR group was significantly greater than that in the control group. DAB chromogenization, ×400

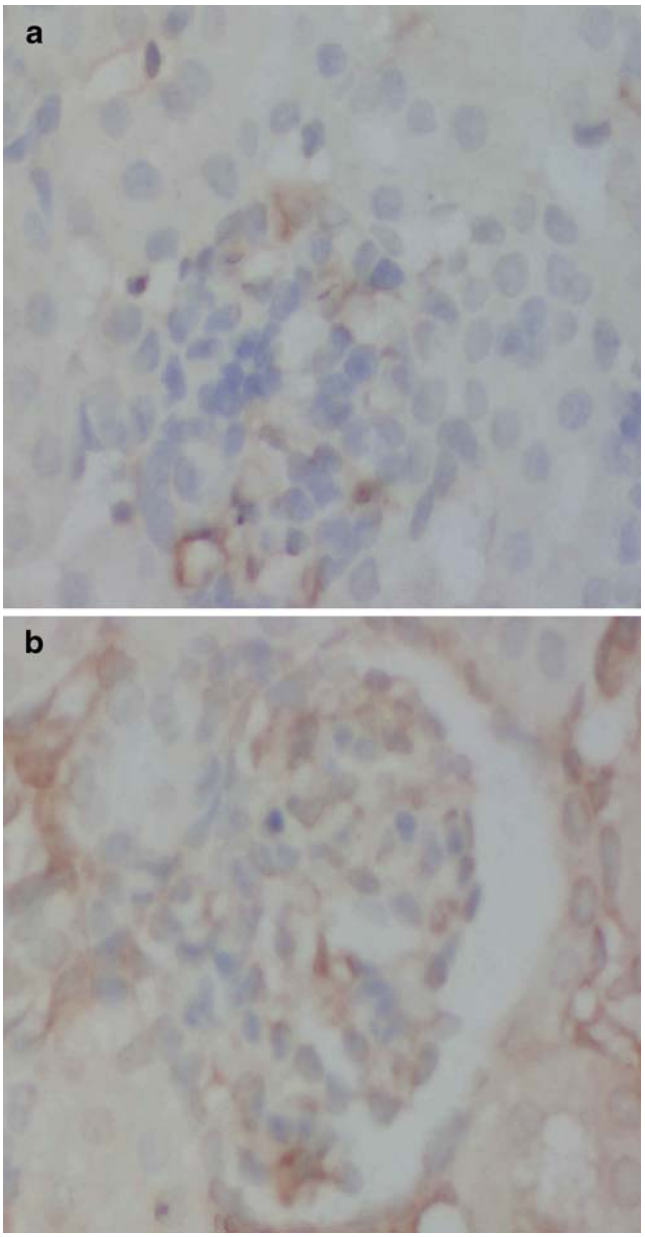

Fig. 5 IHC analysis of perlecan expression in the kidneys. **a** IUGR group; **b** control group. Perlecan was expressed in both the glomeruli and the tubules. The staining in the IUGR group was significantly lower than that in the control group. DAB chromogenization, ×400

while, in diabetic patients and animals, perlecan is reduced in the renal parenchyma [34]. Our result indicated that perlecan was significantly reduced in the glomeruli of the IUGR group when compared with the control group. Previous study has shown that the deficiency of perlecan leads to the metanephric dysmorphogenesis and consequent atrophy of the mesenchyme exhibiting accelerated apoptosis [35]. Therefore, we speculated that perlecan might play multiple developmental roles, by concentrating growth factors and morphogens near the cell surface and by restricting their subsequent diffusion, and might play a crucial role in the modulation of apoptosis in nephrogenesis.

Besides vimentin and perlecan, we identified 19 other differentially expressed proteins that play important roles in energy metabolism, oxidation and reduction, signal transduction, cell proliferation and apoptosis. Transketolase is an important enzyme in the pentose phosphate pathway, a pathway responsible for the generation of reducing equivalents and which is essential for energy transduction, and transketolase may have important implications in nutrition [36, 37]. A 75 kDa glucose-regulated protein is known to be induced under conditions of low glucose levels and nutritional and other environmental stress. A previous study has revealed increased levels of 75 kDa glucose-regulated protein in ischemic brain [38]. Apolipoprotein A-IV acts as a satiety signal and is regulated by nutritional and metabolic stress. A previous study has shown that the starving of mice for 24 h led to increased levels of liver and ileal apolipoprotein A-IV mRNA and plasma apolipoprotein A-IV protein [39]. Our results indicated that transketolase, 75 kDa glucose-regulated protein and apolipoprotein A-IV were significantly increased in the IUGR group when compared to the control group. It is, therefore, tempting for one to presume that these proteins might protect the tissue from metabolic stress such as nutrition deprivation. In addition, methylmalonate-semialdehyde dehydrogenase catalyzes the irreversible oxidative decarboxylation of malonate semialdehyde and methylmalonate semialdehyde to acetyl-coenzyme A (CoA) and propionyl-CoA, and delta 1-pyrroline-5-carboxylate dehydrogenase might be a regulatory enzyme in the ornithine–glutamate pathway [40, 41]. These two enzymes are involved primarily in oxidation and reduction, and high concentrations of these enzymes may alter the cellular redox state in nephrogenesis. Meanwhile, retinal dehydrogenases convert retinal into retinoic acids, which are important signaling molecules in embryogenesis and tissue differentiation [42]. Heterogeneous nuclear ribonucleoprotein K has been implicated in chromatin remodeling, transcription, splicing, and translation processes. Previous data have demonstrated that heterogeneous nuclear ribonucleoprotein K may promote cell proliferation and have a negative effect on the promotion of differentiation in vivo [43]. Elevated levels of these two proteins may alter cellular signaling and cell proliferation, impairing nephrogenesis. Furthermore, Rho GDP dissociation inhibitor is a cellular regulatory protein and an anti-apoptotic molecule that acts primarily by controlling cellular distribution. Previous data have demonstrated that cardiac-specific overexpression of Rho GDP dissociation inhibitor disrupts cardiac morphogenesis and inhibits cardiomyocyte proliferation, leading to embryonic lethality [44, 45]. Our results indicated that levels of Rho GDP dissociation inhibitor were significantly increased in the IUGR group and suggested that overexpression of this protein might alter apoptosis and disrupt renal morphogenesis.

Our results on the differential kidney protein profiles can be compared with the results of a recent study on the effect of IUGR on the proteomes of the small intestine, liver and skeletal muscle in newborn piglets [46]. The results of that study showed that desmin, cytoskeletal β-actin, the immunoglobulin (Ig) α chain C region, and creatine kinase β-type, etc. were differentially expressed in the small intestine, while transferrin, ζ-crystallin, and alcohol dehydrogenase, etc. were differentially expressed in the liver. Meanwhile, apolipoprotein A1, peroxiredoxin 1, and the tubulin β-chain, etc. were differentially expressed in skeletal muscle. This suggests that IUGR caused completely different proteome changes in various neonatal organs, implying that multiple mechanisms might be involved in IUGR-associated deficiencies in organ development.

In conclusion, a comparative proteomic approach has provided new clues for future research. Data from this study may provide, at least partly, evidence that abnormality of metabolism, imbalance of redox and apoptosis, and disorder of cellular signal and cell proliferation may be the major mechanisms responsible for abnormal nephrogenesis in IUGR. More detailed investigations, including protein expression, action mechanism and protein interaction, are needed to uncover the pathogenic mechanism causing abnormal nephrogenesis in IUGR.

Acknowledgements This research was funded by the National Natural Science Foundation of China (NSFC, 30672242). We are grateful to Xiu-Rong Zhang and Zhong-Hua Zhao for their technical assistance.

References

1. Barker DJ, Gluckman PD, Godfrey KM, Harding JE, Owens JA, Robinson JS (1993) Fetal nutrition and cardiovascular disease in adult life. Lancet 341:938–941
2. Armitage JA, Taylor PD, Poston L (2005) Experimental models of developmental programming: consequences of exposure to an energy rich diet during development. J Physiol 565:3–8
3. Silver LE, Decamps PJ, Korst LM, Platt LD, Castro LC (2003) Intrauterine growth restriction is accompanied by decreased renal volume in the human fetus. Am J Obstet Gynecol 188:1320–1325

4. Latini G, De Mitri B, Del Vecchio A, Chitano G, De Felice Z, Zetterström R (2004) Foetal growth of kidneys, liver and spleen in intrauterine growth restriction: "programming" causing "metabolic syndrome" in adult age. Acta Paediatr 93:1635–1639
5. Rodríguez-Soriano J, Aguirre M, Oliveros R, Vallo A (2005) Long-term renal follow-up of extremely low birth weight infants. Pediatr Nephrol 20:579–584
6. Hoy WE, Rees M, Kile E, Mathews JD, Wang Z (1999) A new dimension to the Barker hypothesis: low birthweight and susceptibility to renal disease. Kidney Int 56:1072–1077
7. Chen J, Xu H, Shen Q, Guo W, Sun L, Lin SY (2006) Influence of intrauterine growth retardation on blood pressure and renal function in rats. Zhanghua Shen Zang Bing Za Zhi 22:706–707
8. Godfrey KM, Barker DJ (2000) Fetal nutrition and adult disease. Am J Clin Nutr 71:1344S–1352S
9. Martins JP, Monteiro JC, Paixão AD (2003) Renal function in adult rats subjected to prenatal dexamethasone. Clin Exp Pharmacol Physiol 30:32–37
10. Mañalich R, Reyes L, Herrera M, Melendi C, Fundora I (2000) Relationship between weight at birth and the number and size of renal glomeruli in humans: a histomorphometric study. Kidney Int 58:770–773
11. Thame M, Osmond C, Wilks RJ, Bennett FI, McFarlane-Anderson N, Forrester TE (2000) Blood pressure is related to placental volume and birth weight. Hypertension 35:662–667
12. Wu G, Bazer FW, Cudd TA, Meininger CJ, Spencer TE (2004) Maternal nutrition and fetal development. J Nutr 134:2169–2172
13. Sahajpal V, Ashton N (2003) Renal function and angiotensin AT1 receptor expression in young rats following intrauterine exposure to a maternal low-protein diet. Clin Sci 104:607–614
14. do Carmo Pinho Franco M, Nigro D, Fortes ZB, Tostes RC, Carvalho MH, Lucas SR, Gomes GN, Coimbra TM, Gil FZ (2003) Intrauterine undernutrition—renal and vascular origin of hypertension. Cardiovasc Res 60:228–234
15. Alexander BT (2003) Intrauterine growth restriction and reduced glomerular number: role of apoptosis. Am J Physiol Regul Integr Comp Physiol 285:R933–R934
16. Pham TD, MacLennan NK, Chiu CT, Laksana GS, Hsu JL, Lane RH (2003) Uteroplacental insufficiency increases apoptosis and alters p53 gene methylation in the full-term IUGR rat kidney. Am J Physiol Regul Integr Comp Physiol 285:962–970
17. Arthur JM, Thongboonker V, Scherzer JA, Cai J, Pierce WM, Klein JB (2002) Differential expression of proteins in renal cortex and medulla: a proteomic approach. Kidney Int 62:1314–1321
18. Thongboonker V, Barati MT, McLeish KR, Benarafa C, Remold-O'Donnell E, Zheng S, Rovin BH, Pierce WM, Epstein PN, Klein JB (2004) Alterations in the renal elastin-elastase system in type 1 diabetic nephropathy identified by proteomic analysis. J Am Soc Nephrol 15:650–662
19. Thongboonker V (2004) Proteomics in nephrology: current status and future directions. Am J Nephrol 24:360–378
20. Schaub S, Rush D, Wilkins J, Gibson IW, Weiler T, Sangster K, Nicolle L, Karpinski M, Jeffery J, Nickerson P (2004) Proteomic-based detection of urine proteins associated with acute renal allograft rejection. J Am Soc Nephrol 15:219–227
21. Weinkauf M, Hiddemann W, Dreyling M (2006) Sample pooling in 2-D gel electrophoresis: a new approach to reduce nonspecific expression background. Electrophoresis 27:4555–4558
22. Karp NA, Lilley KS (2009) Investigating sample pooling strategies for DIGE experiments to address biological variability. Proteomics 9:388–397
23. Jia SQ, Niu ZJ, Zhang LH, Zhong XY, Shi T, Du H, Zhang GG, Hu Y, Su XL, Ji JF (2009) Identification of prognosis-related proteins in advanced gastric cancer by mass spectrometry-based comparative proteomics. J Cancer Res Clin Oncol 135:403–411
24. Ivaska J, Pallari HM, Nevo J, Eriksson JE (2007) Novel functions of vimentin in cell adhesion, migration, and signaling. Exp Cell Res 313:2050–2062
25. Murer L, Benetti E, Centi S, Della Vella M, Artifoni L, Capizzi A, Zucchetta P, Del Prete D, Carasi C, Montini G, Rigamonti W, Zaccello G (2006) Clinical and molecular markers of chronic interstitial nephropathy in congenital unilateral ureteropelvic junction obstruction. J Urol 176:2668–2673
26. Sanai T, Sobka T, Johnson T, el-Essawy M, Muchaneta-Kubara EC, Ben Gharbia O, el Oldroyd S, Nahas AM (2000) Expression of cytoskeletal proteins during the course of experimental diabetic nephropathy. Diabetologia 43:91–100
27. Bob FR, Gluhovschi G, Herman D, Potencz E, Gluhovschi C, Trandafirescu V, Schiller A, Petrica L, Velciov S, Bozdog G, Vernic C (2008) Histological, immunohistochemical and biological data in assessing interstitial fibrosis in patients with chronic glomerulonephritis. Acta Histochem 110:196–203
28. Kim YH, Goyal M, Kurnit D, Wharram B, Wiggins J, Holzman L, Kershaw D, Wiggins R (2001) Podocyte depletion and glomerulosclerosis have a direct relationship in the PAN-treated rat. Kidney Int 60:957–968
29. Zou J, Yaoita E, Watanabe Y, Yoshida Y, Nameta M, Li H, Qu Z, Yamamoto T (2006) Upregulation of nestin, vimentin, and desmin in rat podocytes in response to injury. Virchows Arch 448:485–492
30. Lucas SR, Miraglia SM, Zaladek Gil F, Machado Coimbra T (2001) Intrauterine food restriction as a determinant of nephrosclerosis. Am J Kidney Dis 37:467–476
31. Knox SM, Whitelock JM (2006) Perlecan: how does one molecule do so many things? Cell Mol Life Sci 63:2435–2445
32. Whitelock JM, Melrose J, Iozzo RV (2008) Diverse cell signaling events modulated by perlecan. Biochemistry 47:11174–11183
33. Björnson Granqvist A, Ebefors K, Saleem MA, Mathieson PW, Haraldsson B, Nyström JS (2006) Podocyte proteoglycan synthesis is involved in the development of nephrotic syndrome. Am J Physiol Renal Physiol 291:F722–F730
34. Ha TS, Song CJ, Lee JH (2004) Effects of advanced glycosylation endproducts on perlecan core protein of glomerular epithelium. Pediatr Nephrol 19:1219–1224
35. Kanwar YS, Liu ZZ, Kumar A, Usman MI, Wada J, Wallner EI (1996) D-glucose-induced dysmorphogenesis of embryonic kidney. J Clin Invest 98:2478–2488
36. Alexander-Kaufman K, Harper C (2009) Transketolase: observations in alcohol-related brain damage research. Int J Biochem Cell Biol 41:717–720
37. Zhao J, Zhong CJ (2009) A review on research progress of transketolase. Neurosci Bull 25:94–99
38. Krishna SB, Alfonso LF, Thekkumkara TJ, Abbruscato TJ, Bhat GJ (2007) Angiotensin II induces phosphorylation of glucose-regulated protein-75 in WB rat liver cells. Arch Biochem Biophys 457:16–28
39. Hanniman EA, Lambert G, Inoue Y, Gonzalez FJ, Sinal CJ (2006) Apolipoprotein A-IV is regulated by nutritional and metabolic stress: involvement of glucocorticoids, HNF-4 alpha, and PGC-1 alpha. J Lipid Res 47:2503–2514
40. Kedishvili NY, Goodwin GW, Popov KM, Harris RA (2000) Mammalian methylmalonate-semialdehyde dehydrogenase. Methods Enzymol 324:207–218
41. Wong PT, Leong SF (1985) Delta-1-pyrroline-5-carboxylate dehydrogenase, a possible regulatory enzyme in transmitter glutamic acid metabolism—a preliminary report. Ann Acad Med Singapore 14:143–146
42. Gagnon I, Duester G, Bhat PV (2003) Enzymatic characterization of recombinant mouse retinal dehydrogenase type 1. Biochem Pharmacol 65:1685–1690
43. Wei CC, Zhang SL, Chen YW, Guo DF, Ingelfinger JR, Bomsztyk K, Chan JS (2006) Heterogeneous nuclear ribonucleoprotein K

modulates angiotensinogen gene expression in kidney cells. J Biol Chem 281:25344–25355
44. Zhang B, Zhang Y, Dagher MC, Shacter E (2005) Rho GDP dissociation inhibitor protects cancer cells against drug-induced apoptosis. Cancer Res 65:6054–6062
45. Wei L, Imanaka-Yoshida K, Wang L, Zhan S, Schneider MD, DeMayo FJ, Schwartz RJ (2002) Inhibition of Rho family GTPases by Rho GDP dissociation inhibitor disrupts cardiac morphogenesis and inhibits cardiomyocyte proliferation. Development 129:1705–1714
46. Wang J, Chen L, Li D, Yin Y, Wang X, Li P, Dangott LJ, Hu W, Wu G (2008) Intrauterine growth restriction affects the proteomes of the small intestine, liver, and skeletal muscle in newborn pigs. J Nutr 138:60–66